Calculation of Fishing Net Drag

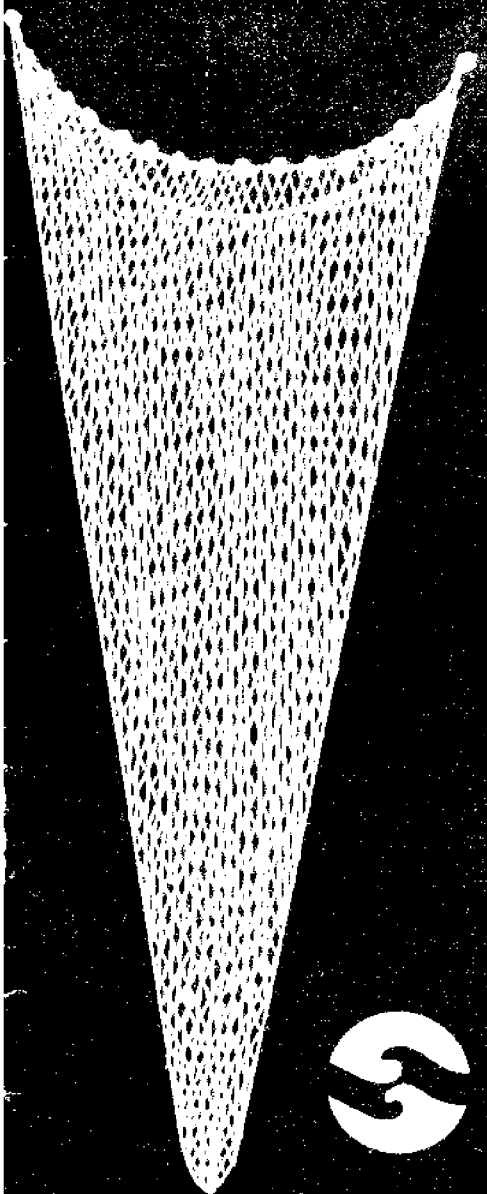

T. Kowalski
J. Giannotti

Ocean Engineering
Sea Grant

University of Rhode Island
Marine Technical Report No. 15

CALCULATION OF FISHING NET DRAG

T. Kowalski

J. Giannotti

Ocean Engineering

Sea Grant

University of Rhode Island

Marine Technical Report No. 15

Kingston 1974

Additional copies of Marine Technical Report Number 15 are available from the Marine Advisory Service, University of Rhode Island, Narragansett Bay Campus, Narragansett, Rhode Island 02882.

CONTENTS

TABLES

FIGURES

Introduction

Fishing is one of the oldest occupations, providing man with his basic food requirements over the ages. However, the tools of the trade have remained almost unchanged. Except for the introduction of power for the propulsion of fishing vessels and winches and improved, new materials for the construction of trawls, the methods of fishing and the design of fishing gear have remained substantially unchanged.

Looking at fishing net design and construction, the basic mesh units have remained the same too since ancient times. Recently, together with the use of artificial fibers, so-called knotless construction has been introduced into the manufacture of fishing nets. However, the worth of these knotless nets still has not been scientifically proven and the main thrust of improvements has been in the design of the shape of the trawl, the doors, and the floats.

Today there exists a great number of trawl designs, and almost every fisherman modifies one of the standard trawls for his particular use. However, these modifications are made on the basis of personal preference and experience on a trial-and-error basis. There is no scientific proof that each modified trawl is the optimum for the particular boat and fishing task. On the contrary, it is almost certain that an improved trawl could be designed in each case. Such designs could be based on the assumption that each trawl is assembled from a number of basic parts, each one analyzed separately, and the complete trawl performance is the sum of the performance of all the components. But this is possible only if the performance characteristics of the trawl component parts are available.

To summarize, the optimum performance of fish trawling operations depends to a large degree on efficient fishing gear, and, to determine efficiency, it is necessary to analyze each component of the gear. For example, one of these basic components is the net for which there is very little information available regarding its drag. There are two possible approaches that can be taken to determine the drag of a net: one is to measure experimentally the drag of a net model or of a full-size net. The second is to theoretically calculate the drag by adding

together the drag of each basic component of the total net. Both of these approaches have been used in this study.

Experimental Procedures and Apparatus

Experiments were performed in a wind tunnel due to the ease this method provides in handling the nets. Some tests were also run in a water towing tank to check the validity of the air tests. Tests of flat panels were run first to obtain basic drag coefficients required for later theoretical calculations.

The criterion for establishing wind velocities in the wind tunnel was Reynolds number similarity. The most significant forces acting on a trawl at fairly large depths are the frictional forces (associated with viscosity, velocity, and size) and the dynamic forces (associated with density and velocity). Since the trawl operates far away from the ocean surface, and gravitational forces are not important, there is no need to account for Froude number effects. Furthermore, the small velocities involved in trawling make it unnecessary to look at the effects of cavitation number and Mach number.

The twine of the nets used in the tests was kept at its full-scale size and consequently the only requirement for dynamic similarity was that the ratios of velocity to kinematic viscosity of the fluid be the same. This was achieved in the wind tunnel with relatively high wind velocities.

The drag force on the netting panels was measured by means of a Strain Gage Balance designed to support test models in a wind tunnel. In addition, the angle of attack of the support base could be adjusted over a 0° to 90° range. The netting panels were attached to rectangular frames made up of thin aluminum bars with rounded edges. These framed panels were then bolted to a more rigid streamlined frame which was fixed to the support base of the balance. Figure 1 shows the measuring apparatus next to the wind tunnel with a netting panel ready for testing.

The drag calibration was carried out by applying a horizontal pull in the longitudinal direction and using known weights attached to a cord running from the model support base and through a pulley. The lift calibration was carried out by placing weights and a curve was plotted in each case. These curves are shown in figure 2. Both plots were essentially straight lines indicating that, in the range of loads of interest, there was a linear relationship between the reading in microvolts and the measured loads.

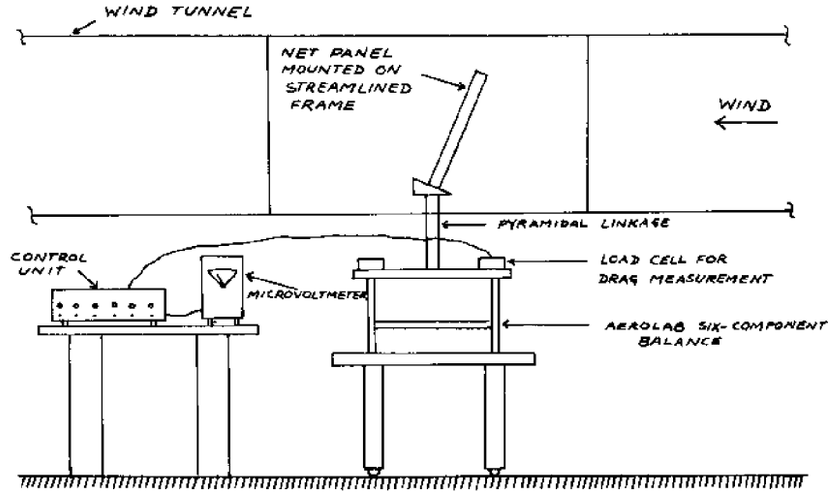

Figure 1. Experimental setup used for measuring fishing net drag.

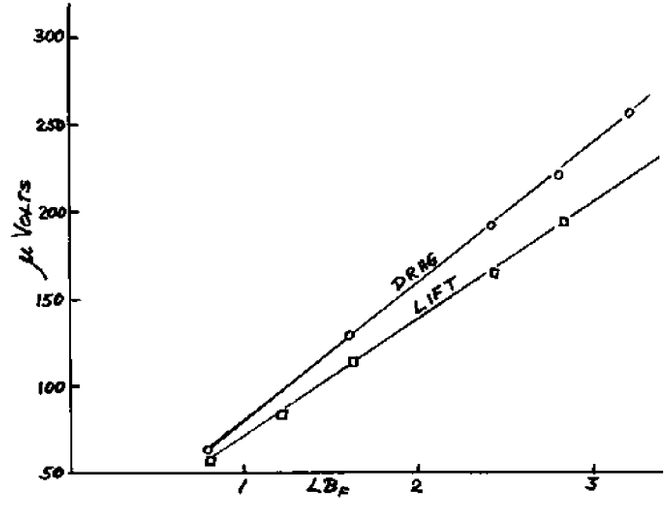

Figure 2. Lift calibration of the aerolab pyramidal strain gage balance.

Data Collection and Analysis

Before conducting tests, two important things had to be considered. The first was the selection of types of netting similar to those used in common commercial applications and the second was to determine the wind speed range that would yield the Reynolds numbers corresponding to those achieved in actual trawling operations.

Point Judith (Rhode Island) trawlers use bottom trawls in the majority of their operations. These are either of standard or local design and most of them are similar to the trawls of the Yankee series and the Granton type. Consequently, it was decided to establish the geometry of the nets to be tested on the basis of these two major classifications. Table 1 gives the range of net mesh sizes used in the manufacture of the Granton and Yankee trawls. This information corresponds to bottom trawls tested in full scale at sea by P.J.G. Carrothers et al (1969). Two mesh sizes were selected from available commercial nets; these are 2.75 inches and 4.75 inches, both of which fall within the range of interest according to table 1.

Based on personal communication with local fishermen, we set the range of trawling speeds between 2 and 3 knots. The Reynolds number of a net is defined as $N_R = VL_b/\nu$ where L_b is the length of a "bar" (a mesh is made up of four bars), V is the trawling speed or wind speed, and ν is the kinematic viscosity of water or air. Since L_b is the same in the model as it is in full-scale, the only requirement for dynamic similarity is that the ratio of velocity to kinematic viscosity be the same for the net whether subjected to the action of the wind in the wind tunnel or to the action of seawater flowing past the net. At an average water temperature of 59° F the

Table 1. Range of net mesh sizes used in trawls studied.

Trawl Type	Largest Mesh Size	Smallest Mesh Size
Yankee 35	5 in	4.5 in
Yankee 36	5 in	4.5 in
Yankee 41.5	5 in	4.5 to 3.5 in
Yankee 41	5 in	4.5 to 2.75 in
Granton	5.5 in	4.5 in

kinematic viscosity of salt water is 1.2817×10^{-5} ft^2/ sec, and at an average wind tunnel temperature of 80° F (actual testing condition) the kinematic viscosity of air is 1.69×10^{-4} ft^2/sec. A trawling speed of 2 knots or 3.38 ft/sec in salt water at 59° F requires a wind speed of 44.6 ft/sec at 80° F in the wind tunnel. Similarly, a trawling speed of 3 knots or 5.07 ft/sec requires a wind speed of 66.9 ft/sec in the wind tunnel. The coefficient of drag, C_D, of a netting panel is defined as

$$C_D = D/1/2\ \rho\ V^2 A_p$$

where D is the drag force in lbf, ρ is the fluid density in slugs/ft^3, V is the flow velocity in ft/sec, and A_p is the projected solid area of a netting panel in ft^2. The magnitude of A_p is computed by adding up the projected areas of each bar and each knot that make up the rectangular netting panel. The angle of attack, α, of a panel, with respect to the flow, is defined so that $\alpha = 90°$ when the panel is perpendicular to the flow, and $\alpha = 0°$ when the panel is parallel to the flow. Figure 3 shows a simplified diagram of a mesh where the bars are drawn as cylinders of length L_b and diameter D_b, and the knots are represented by spheres of diameter D_k. The magnitude of A_p is given by

$$A_p = (b \times L_b \times D_b) + k \times \pi \times D_k^2/4) \qquad (1)$$

where b is the total number of bars and k is the total number of knots in a panel.

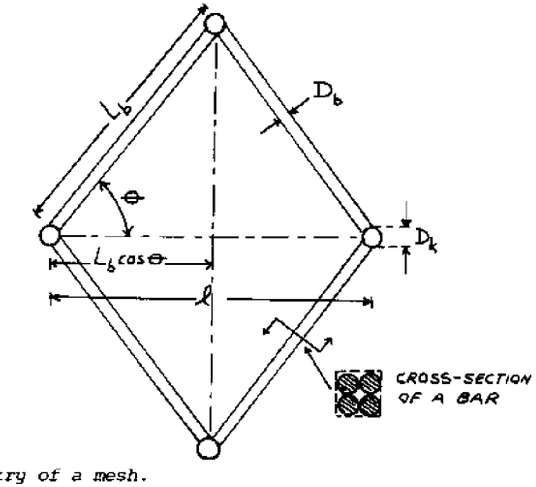

Figure 3. Geometry of a mesh.

To obtain the variation of the coefficient of drag from the angle of attack, α, each panel was tested at angles ranging between 90° and 5° and at wind speeds between 20 ft/sec and 70 ft/sec.

Prior to testing the panels, the drag and lift forces acting on the frames without the nets were measured over the same range of wind speeds and angles of attack. These measurements were subtracted from the readings obtained with the nets attached to the frames. The result was the actual drag force acting on the net alone. Interference by the frame was assumed to be negligible.

Tables 2 and 3 show the geometric characteristics of nets A and B. Tables 4 and 5 contain the values of C_D as a function of the Reynolds number and angle of attack for both nets. Figures 4 and 5 are plots of C_D versus the Reynolds number for different values of α for each panel tested.

The curves of C_D versus Reynolds number for different values of the angle of attack indicate that the coefficient of drag at a given angle of attack remains essentially constant in the range of Reynolds numbers between 4.5 and 10^4 and 8×10^4 for net A, and between 2.5×10^4 and 4.5×10^4 for net B.

Since the range of trawling speeds of interest lies between 2 and 3 knots, the corresponding minimum values of the Reynolds number is about 5.6×10^4 for the 4.75-inch mesh and about 3.2×10^4 for the 2.75-inch mesh. Consequently, only those values of C_D corresponding to Reynolds numbers greater than these minima were considered in subsequent analyses.

The coefficient of drag of the net panels remains approximately constant in the range of Reynolds numbers of interest. Therefore, an arithmetic average of the values given in tables 4 and 5 at each angle of attack was calculated. The $\bar{C}_D$ for the 4.75-inch mesh net was computed from the values of C_D corresponding to Reynolds numbers of 4.684×10^4 and above. Similarly, the $\bar{C}_D$ for the 2.75-inch mesh net values corresponded to 2.712×10^4 and above. The values obtained in this manner for each angle of attack are given in table 6. Figures 6 and 7 are corresponding plots of $\bar{C}_D$ versus α.

From the plots of $\bar{C}_D$ versus α it was observed that, at least in the range of interest, the experimental points followed a sinusoidal pattern of the form

$$\bar{C}_D = \bar{C}_{D90^{\circ}} (\sin \alpha) + 0.005 \qquad (2)$$

Table 2. Net A.

Size of Net Panel	20 in x 22 in
Bar Length, (L_b)	2.375 in
Mesh	4.75 in
Bar Diameter, (D_b)	0.0625 in
Knot Diameter, (D_k)	0.1875 in
Number of Knots, (k)	70
Number of Bars, (b)	162
Projected Area of a Net Panel, (α =90°)	25.98 in^2
$\theta = 60^{\circ}$	

Table 3. Net B.

Size of Net Panel	20 in x 22 in
Bar Length, (L_b)	1.375 in
Mesh	2.75 in
Bar Diameter, (D_b)	0.0625 in
Knot Diameter, (D_k)	0.1875 in
Number of Knots, (k)	209
Number of Bars, (b)	450
Projected Area of a Net Panel, (α = 90°)	44.41 in^2
$\theta = 60^{\circ}$	

Table 4. C_D values.

Net A

$N_R = 2.342 \times 10^4$		$N_R = 3.513 \times 10^4$	
α°	C_D	α°	C_D
90	2.322	90	2.058
60	1.477	60	1.620
30	0.608	30	0.676
15	0.122	15	0.406
10	0.377	10	0.476
5	0.304	5	0.070

$N_R = 4.684 \times 10^4$		$N_R = 5.855 \times 10^4$	
α°	C_D	α°	C_D
90	1.720	90	1.532
60	1.256	60	1.556
30	0.836	30	1.118
15	0.268	15	0.244
10	0.116	10	0.220
5	0.152	5	0.098

$N_R = 7.026 \times 10^4$		$N_R = 7.904 \times 10^4$	
α°	C_D	α°	C_D
90	1.740	90	1.760
60	1.638	60	1.588
30	1.166	30	0.988
15	0.304	15	0.280
10	0.220	10	0.214
5	0.136	5	0.186

Table 5. C_D values.

Net B

$N_R = 1.365 \times 10^4$		$N_R = 2.034 \times 10^4$	
α°	C_D	α°	C_D
90	2.176	90	2.174
60	1.693	60	1.817
30	0.932	30	0.910
15	0.356	15	0.395
10	0.313	10	0.474
5	0.270	5	

$N_R = 2.712 \times 10^4$		$N_R = 3.39 \times 10^4$	
α°	C_D	α°	C_D
90	1.800	90	1.849
60	1.555	60	1.693
30	0.956	30	1.109
15	0.311	15	0.398
10	0.334	10	0.398
5	0.167	5	0.214

$N_R = 4.068 \times 10^4$		$N_R = 4.577 \times 10^4$	
α°	C_D	α°	C_D
90	1.906	90	1.795
60	1.718	60	1.717
30	1.185	30	1.085
15	0.790	15	0.406
10	0.415	10	0.429
5	0.208	5	0.218

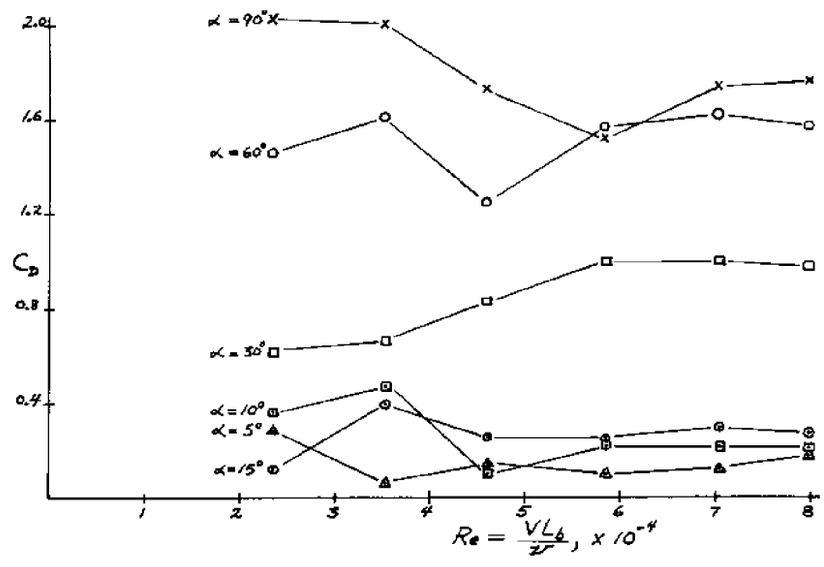

Figure 4. C_D vs. Reynolds number for different angles of attack: net A.

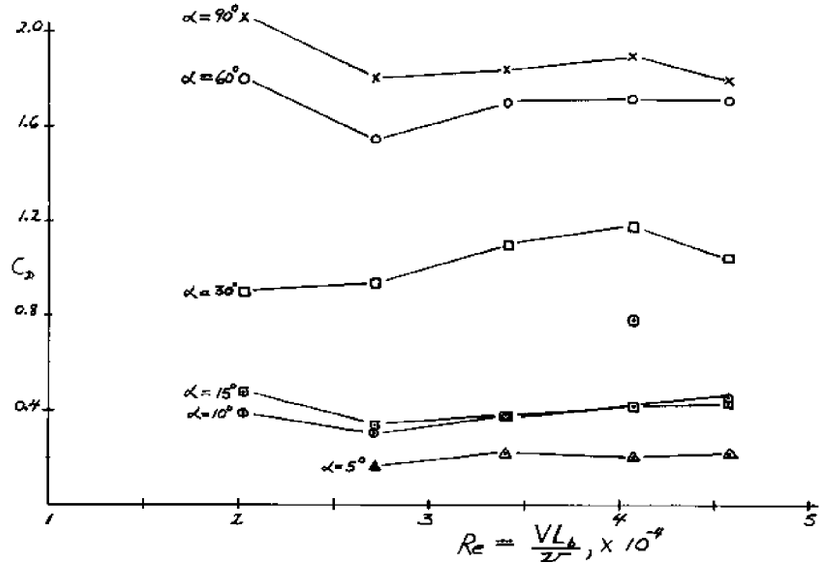

Figure 5. C_D vs. Reynolds number for different angles of attack: net B.

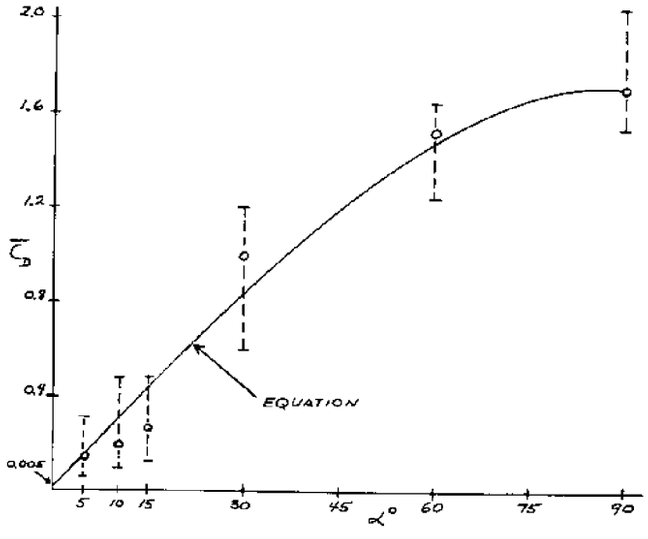

Figure 6. $\bar{C}_D$ vs. angle of attack: net A.

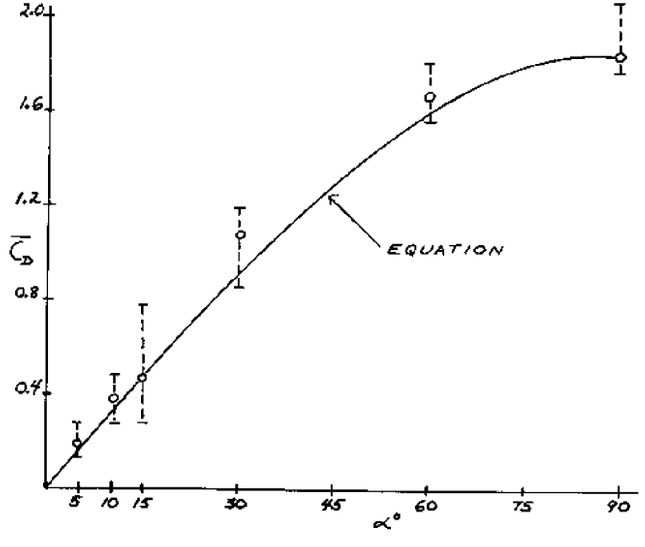

Figure 7. $\bar{C}_D$ vs. angle of attack: net B.

Table 6. Average coefficient of drag.

	Net A	Net B
α°	$\bar{C}_D$	$\bar{C}_D$
90	1.70	1.84
60	1.51	1.67
30	1.03	1.08
15	0.27	0.48
10	0.19	0.39
5	0.14	0.20

where $\bar{C}_{D90}$ is the average coefficient of drag when the nets are perpendicular to the flow and $\bar{C}_D$ is the average coefficient of drag at any value of α between 5° and 90°. The curves obtained using equation 2 are shown in figures 6 and 7. The constant term in equation 2 represents the coefficient of frictional drag and it is determined from the intercept at $\alpha = 0^\circ$.

Coefficient of Drag from Knotless Nets

Wind tunnel tests were also conducted on netting panels made of knotless nets in order to measure their coefficient of drag. The netting geometry is given in table 7. The measured values of C_D are given in table 8 as a function of the Reynolds number (based on the length of the bars) and angle of attack. Table 9 gives the average coefficient of drag, which is computed in the same manner as for the conventional nets. Figure 8 shows curves of C_D versus the Reynolds number at different values of angle of attack. These two plots indicate that, in the range of speeds considered, C_D can be taken to remain constant with the Reynolds number. Figure 9 shows curves of $\bar{C}_D$ versus α based on the experimental values and on equation 2.

The comparison with conventional nets shows that knotless netting has lower drag coefficients at higher angles of attack, but at smaller angles the advantage disappears. Since most netting in a trawl is operating at small angles of attack, there does not seem to be any advantage in using knotless netting to improve drag.

Table 7. Geometrical characteristics of the knotless net panel.

Size of Net Panel	20 in x 22 in
Bar Length, (L_b)	0.875 in
Bar Diameter, (D_b)	0.0937 in
Knot Length, (L_k)	0.3125 in
Knot Width, (B_k)	0.1560 in
Number of Knots, (k)	412
Number of Bars, (b)	880
Projected area of a net Panel, ($\alpha = 90^{\circ}$)	92.23 in^2

Table 8. Coefficient of drag as a function of Reynolds number and angle of attack for the knotless net panel.

$N_R = 0.862 \times 10^4$

α°	C_D
90	2.322
30	0.599
20	0.592
15	0.563
10	0.513
5	0.162

$N_R = 1.293 \times 10^4$

α°	C_D
90	2.102
30	0.811
20	0.600
15	0.499
10	0.417
5	0.095

$N_R = 1.724 \times 10^4$

α°	C_D
90	1.904
30	0.853
20	0.588
15	0.408
10	0.313
5	0.160

$N_R = 2.155 \times 10^4$

α°	C_D
90	1.624
30	0.968
20	0.568
15	0.425
10	0.334
5	0.180

$N_R = 2.586 \times 10^4$

α°	C_D
90	1.569
30	1.003
20	0.588
15	0.460
10	0.319
5	0.137

$N_R = 2.909 \times 10^4$

α°	C_D
90	1.477
30	1.008
20	0.575
15	0.417
10	0.335
5	0.164

Table 9. Average coefficient of drag for the knotless net and comparison with nets A and B.

	$\bar{C}_D$		
α°	Knotless	Net A	Net B
90	1.64	1.70	1.84
30	0.96	1.03	1.08
20	0.58	----	----
15	0.43	0.27	0.48
10	0.33	0.19	0.39
5	0.16	0.14	0.20

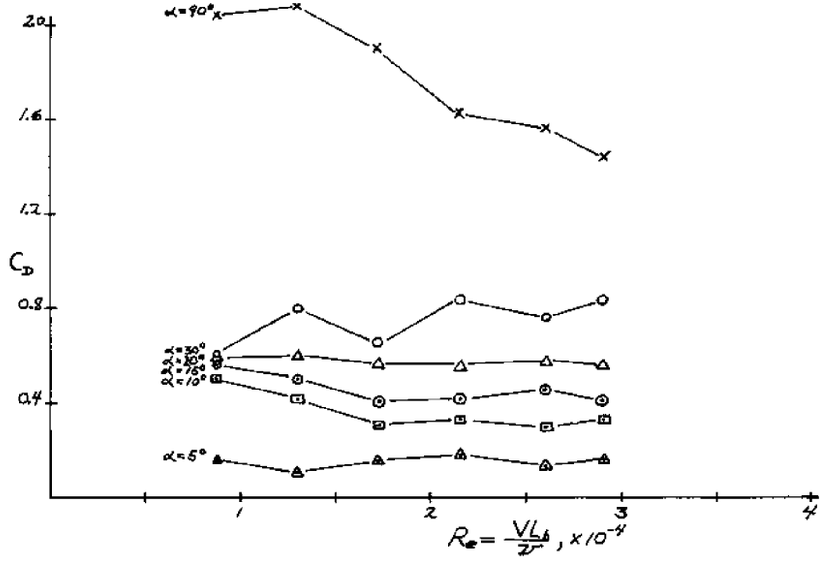

Figure 8. C_D vs. Reynolds number for different angles of attack: knotless net.

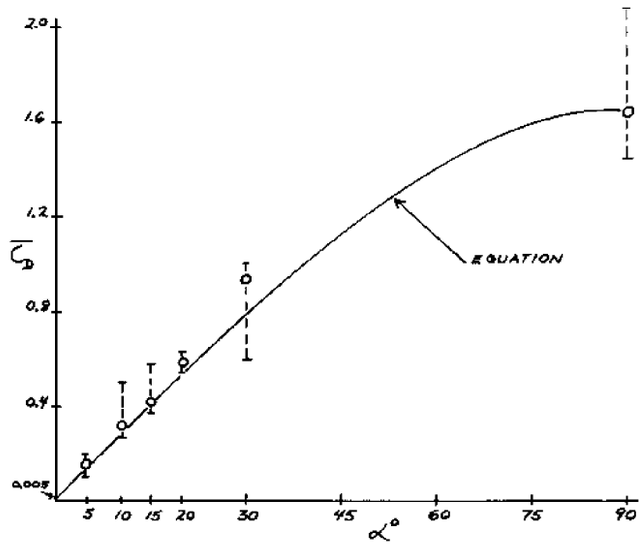

Figure 9. $\bar{C}_D$ vs. angle of attack: knotless net.

Theoretical Estimate of Fishing Net Drag

It was found that the value of $\bar{C}_D$ depended on $\bar{C}_{D90°}$ and α. Equation 2 implies that if $\bar{C}_{D90°}$ and α are known, then the coefficient of drag at any angle of attack can be readily estimated. Furthermore, if $\bar{C}_{D90°}$ can be estimated, then there is no need to conduct any testing in order to calculate $\bar{C}_D$.

If the bars and knots that make up a net panel are represented by cylinders and spheres, respectively, then an analysis can be carried out based on known values of C_D for such geometric shapes.

The projected area A_k of a knot is given by $1/4\,\pi\, D_k^2$ where D_k is the "diameter" of the knot. The projected area of a bar A_b is given by $D_b \times L_b$ where L_b is the length of the bar and D_b is its diameter.

Figure 3 shows that the bars or prisms have basically a diamond-shaped cross-section. Lindsey (1938) gives a value of 2.0 for the coefficient of profile drag of prisms with this particular type of section in the range of Reynolds numbers of interest. In addition, the frictional drag coefficient of 0.02 is added, giving $C_{D\ bar} = 2.02$.

The knots are assumed to be basically spherical and their coefficient of drag, C_{Dk}, is taken from well known curves of C_D for spheres (Hoerner, 1965). In the range of Reynolds numbers of interest the coefficient of drag of a sphere is constant and has a value of 0.47.

The drag force acting on a panel is given by

$$D_{net} = D_{knots} + D_{bars} \qquad (3)$$

where

$$D_{knots} = C_{Dk} \times (A_k k) \times 1/2\ \rho\ V^2 \qquad (4)$$

$$D_{bars} = C_{Db} \times (A_b b) \times 1/2\ \rho\ V^2 \qquad (5)$$

The coefficient of drag $\bar{C}_D$ for the entire panel is then given by $D_{net}/1/2\ \rho\ V^2 A_p$ where $A_p = (A_k k) + (A_b b)$.

$$\bar{C}_{D90°} = \frac{C_{Dk}\ (A_k k) + C_{Db}\ (A_b b)}{A_p} \qquad (6)$$

Equation 6 can be verified by using it to calculate the value of $\bar{C}_{D90°}$ for the nets used in the wind tunnel experiments.

The net with 2.75-inch mesh:

$k = 209$

$b = 450$

$$A_k = \frac{3.1416 \times (0.187)^2}{4 \times 144} = 0.000191 \text{ ft.}^2$$

$$A_b = \frac{0.0625 \times 1.375}{144} = 0.000597 \text{ ft.}^2$$

$C_{Dk} = 0.47$

$C_{Db} = 2.02$

From equation 6

$$\bar{C}_{D90°} = \frac{(0.47 \times 0.000191 \times 209) + (2.02 \times 0.000597 \times 450)}{0.03986 \times 0.2685}$$

$$\bar{C}_{D90^\circ} = 1.82$$

The value of $\bar{C}_{D90^\circ}$ computed from the experimental results is 1.84. A similar calculation for the 4.75-inch mesh net yields a value of 1.72 for the coefficient of drag when the net is perpendicular to the flow. The value computed from the wind tunnel measurements is 1.69.

Equation 6 is not applicable for angles of attack other than 90°. This is due to the interference between bars and the wake effects resulting as the panels are inclined away from the perpendicular.

The coefficient of drag of the nets can be estimated, however, by combining equation 6 for the case when the flow is perpendicular to the nets with the empirical relationship 2 which gives the coefficient of drag as a function of the angle of attack and $\bar{C}_{D90^\circ}$.

$$\bar{C}_D = \frac{C_{Dk}\ (A_k k) + C_{Db}\ (A_b b)}{A_p} \sin \alpha \quad + 0.005 \quad (7)$$

Equation 7 gives the value of the coefficient of drag for any netting panel of known geometry and angle of attack at Reynolds numbers corresponding to trawling speeds between 2 and 3 knots.

The total drag force acting on a netting panel can also be expressed in terms of the surface area of the panel and the solidity of the meshes. The solidity of a mesh is defined as the ratio of the solid area to the surface area of a mesh. Figure 3 shows a schematic diagram of a typical mesh. Recognizing that the contribution of a mesh to a whole panel consists only of two bars and one knot the solid area contributed by a mesh is given by

$$A_{solid} = 2A_b + A_k = (2L_b D_b) + 1/4(\pi D_k^2)$$

The surface area of a mesh is given by

$$A_{surface} = 2L_b^2 \sin\theta \cos\theta$$

By definition solidity is then written as

$$S = \frac{2L_b D_b + 1/4\,\pi D_k^2}{2L_b^2 \cos\theta \sin\theta} \quad (8)$$

The coefficient of drag, $\bar{C}_{D90^\circ}$, is based on the projected solid area of a net which is perpendicular to the flow. Consequently, the total drag force acting on a panel submerged in a flow of velocity V is given by

$$D_{panel} = \bar{C}_{D90^\circ} S (1/2\ \rho\ V^2)\ A_{surface} \quad (9)$$

Summarizing then:

$$D_{panel} = (\bar{C}_{D90^\circ} \sin \alpha + 0.005)\ S\ 1/2\ \rho\ V^2\ A_{surface} \quad (10)$$

where

$$\bar{C}_{D90^\circ} = \frac{C_{Dk}\ (A_k k) + C_{Db}(A_b b)}{A_p} \; ; \; S = \frac{2L_b D_b + 1/4\,\pi D_k^2}{2L_b^2 \cos\theta \sin\theta}$$

$$A_p = (A_k \times k) + (A_b \times b)$$

$$A_k = 1/4\,\pi D_k^2$$

$$C_{Dk} = 0.47$$

$$A_b = D_b \times L_b$$

$$C_{Db} = 2.02$$

Wind Tunnel Tests on Conical Nets

The tests and analyses of the flat net panels can be used directly in applications, such as aquaculture fish pens or purse seining. For trawl nets, however, the drag of curved net panels had to be investigated.

Most of the commercial trawling nets have a large portion which is basically conical in shape. The results obtained for flat panels cannot be applied directly to such geometries without first investigating the nature of the flow past a conical net and measuring the coefficient of drag. Conical nets with circular and elliptical openings were tested in the wind tunnel and in a towing tank. The circular opening had a diameter of 12 inches and a length of 48 inches. The elliptical opening had a major axis of 24 inches and a minor axis of 6 inches, giving the same mouth area as the circular opening.

The ratio of major to minor axes was made to correspond to the ratio of wingspread to headline height in the full-scale trawl. The Yankee trawl series usually operates with a ratio of four. The circular cone was built using a mesh with a size of 4.75 inches and of the same type as the one used in the flat

panel tests. The mesh size was not changed along the cone as is the case in full-scale trawls. The tests were conducted over a range of wind speeds between 40 ft/sec and 70 ft/sec corresponding to trawling speeds of 2 to 3 knots according to Reynolds number similarity. The experimental results are presented in the appendix.

Theoretical Analysis of the Hydrodynamic Drag of Conical Nets

Consider the general cone shape of figure 10 where the major axis is 2b and the minor axis is 2a. The height of the cone is h and α is the angle between the flow V and any generator running from the apex of the cone to the edge of the base opening. The axes, x, y, and z, have their origin at the apex.

The base of the cone is defined by the equation:

$$\frac{x^2}{a^2} + \frac{y^2}{b^2} = \frac{z^2}{h^2} \quad \text{or} \quad y = \frac{bz}{h} \sin t; \; x = \frac{az}{h} \cos t$$

Figure 11 shows a differential element of the surface of the cone. The sides of the element can be expressed in terms of x, y, and z.

$$d\xi = dz/\cos\alpha$$

$$(d\gamma)^2 = (dx)^2 + (dy)^2$$

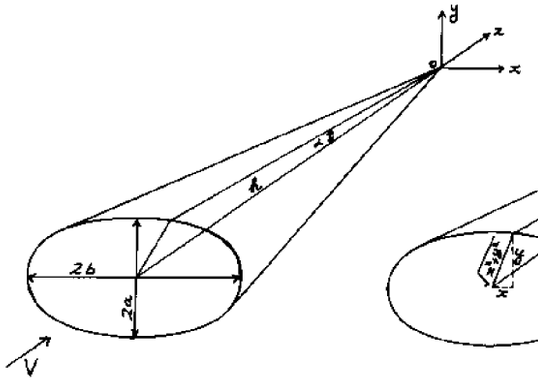

Figure 10. Conical net geometry.

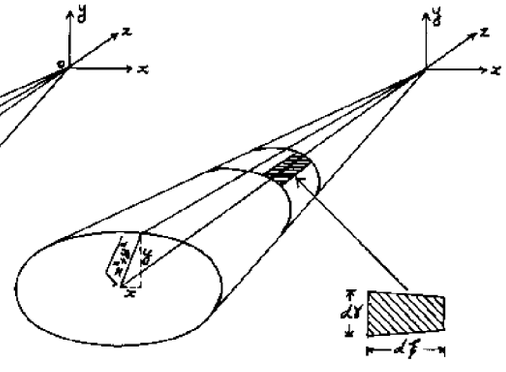

Figure 11. Differential element of a conical net.

Taking the derivative of x and y with respect to t gives

$$dy = \frac{bz}{h} \cos t \, dt$$

and

$$dx = -\frac{az}{h} \sin t \, dt$$

The following expression for $d\gamma$ is thus obtained

$$d\gamma = \frac{bz}{h} \left[1 - \frac{(b^2 - a^2)}{b^2} \sin^2 t\right]^{1/2}$$

From figure 11

$$\cos\alpha = \frac{h}{(h^2 + y^2 + x^2)^{1/2}}$$

Substituting for x^2 and y^2

$$\cos\alpha = \frac{h}{\left(h^2 + \frac{b^2 z^2}{h^2} \sin^2 t - \frac{a^2 z^2}{h^2} \sin^2 t + \frac{a^2 z^2}{h^2}\right)^{1/2}}$$

The cone generators are straight lines so the angle α can be evaluated at z = h giving

$$\cos\alpha = \frac{h}{(h^2 + a^2 - (a^2 - b^2) \sin^2 t)^{1/2}}$$

Multiplying the numerator and the denominator by $(h^2 + a^2)^{1/2}$ gives

$$\cos\alpha = \frac{h/(h^2 + a^2)^{1/2}}{\left(1 - \frac{(a^2 - b^2)}{h^2 + a^2} \sin^2 t\right)^{1/2}}$$

$$d\xi = \frac{dz}{\left(\frac{h^2}{h^2 + a^2}\right)^{1/2} \left(1 - \frac{a^2 - b^2}{h^2 + a^2} \sin^2 t\right)^{1/2}}$$

The coefficient of drag of a net panel inclined at an angle α to the flow is given by equation 2 and the total drag force on a panel is given by 10. Assuming that these two expressions are appli-

cable to small curved panels, the total drag force acting on a conical net can be expressed as

$$D_{cone} = (C_{D90^\circ} \sin \alpha + 0.0005)\ S\ 1/2\ \rho\ V^2 A_{cone}$$

where A_{cone} is the surface area of the cone and is given by the integral.

$$A_{cone} = \int_0^{2\pi} \int_0^{h} d\xi\ d\gamma$$

$$A_{cone} = \int_0^{2\pi} \int_0^{h} \left(\frac{h^2 + a^2}{h^2}\right)^{1/2} \frac{bz}{h} \left(1 - \frac{a^2 - b^2}{h^2 + a^2} \sin^2 t\right)^{1/2} \left(1 - \frac{b^2 - a^2}{b^2} \sin^2 t\right)^{1/2} dz dt$$

$$A_{cone} = \frac{bh}{2} \left(\frac{h^2 + a^2}{h^2}\right)^{1/2} \int_0^{2\pi} \left(1 - \frac{a^2 - b^2}{h^2 + a^2} \sin^2 t\right)^{1/2} \left(1 - \frac{b^2 - a^2}{b^2} \sin^2 t\right)^{1/2} dt$$

Since $\sin \alpha = (1 - \cos^2 \alpha)^{1/2}$

$$\sin \alpha = \frac{\left(\frac{a^2}{h^2 + a^2}\right)^{1/2} \left(1 - \frac{a^2 - b^2}{a^2} \sin^2 t\right)^{1/2}}{\left(1 - \frac{a^2 - b^2}{h^2 + a^2} \sin^2 t\right)^{1/2}}$$

The drag on a conical net becomes

$$D_{cone} = 1/2\ \rho\ V^2 S \left[C_{D90^\circ} \left(\frac{a^2}{h^2 + a^2}\right)^{1/2} (1 - \frac{a^2 - b^2}{a^2} \sin^2 t)^{1/2} \left(1 - \frac{a^2 - b^2}{h^2 + a^2} \sin^2 t\right)^{-1/2} + 0.005\right]$$

$$\frac{bh}{2} \left(\frac{h^2 + a^2}{h^2}\right)^{1/2} \int_0^{2\pi} (1 - \frac{a^2 - b^2}{h^2 + a^2} \sin^2 t)^{1/2}$$

$$(1 - \frac{b^2 - a^2}{b^2} \sin^2 t)^{1/2} \quad dt \qquad (11)$$

The drag force acting on a conical net with a circular opening can be obtained by letting a = b in equation 11.

$$D_{circular\ cone} = 1/2\ \rho\ V^2 S \left[C_{D90^\circ}\ \pi\ a^2 + 0.005\ a\pi (h^2 + a^2)^{1/2}\right] \qquad (12)$$

For an elliptical mouth opening equation 12 can be approximated

$$D_{elliptical\ cone} = 1/2\ \rho\ V^2 S \left[C_{D90^\circ}\ \pi\ ab + 0.005\ (ab)^{1/2} \pi\ (h^2 + ab)^{1/2}\right] \qquad (13)$$

Equation 12 indicates that the drag force acting on a conical net with a circular opening is directly proportional to the solidity of the net, the area of the opening and the coefficient of drag at 90°. Furthermore, equation 12 says that the flow essentially "sees" a circular projected area as it passes through the cone and the aspect ratio of the cone has no effect on the drag. Intuitively the conclusion is not unreasonable since the streamlines remain undisturbed by the conical net. If the cone were solid, the streamline configuration and, consequently, the drag force would be dependent on the aspect ratio of the body.

Conclusions

The research conducted under this project achieved the following results:

1. The feasibility of testing fishing net components and fishing trawl models in a wind tunnel was proved. In these tests artificial fibers were used; hence, the absorption of water by the twine did not have to be considered. The wind tunnel tests are much easier to conduct, can be done much faster and are much cheaper than those conducted in towing tanks.

2. A formula was developed relating the drag of a flat net panel--at any angle of attack to the direction of motion--to the same net panel, at a right angle to the flow of water. Most of the net panels in a trawl are operating at an angle of attack and, thus, their drag can be calculated by testing the required net panels at right angles only. This produces considerable simplification and savings in the test program.

3. An empirical formula has been proposed for calculation of the drag of a net panel subjected to a flow at right angles to the direction of motion, based on a summation of the drags of spheres and cylinders. This will allow the calculation of the drag of a flat net panel, when knowing only the geometry of the netting.

4. A formula was derived for calculation of the drag of a conical trawl net bag, with a circular and elliptical mouth opening, based on the solidity of the netting and the drag coefficient of a flat panel of such netting.

The above achievements will allow the determination of the drag of a net to be obtained either from the approximate empirical formula, based on the drag coefficients of cylinders and spheres, or from actual wind tunnel experiments on models of flat net panels.

The developed facility for testing the fishing nets or their components in the Department of Ocean Engineering at the University of Rhode Island is now available for the fishing industry. One such request to supply a drag coefficient for the design of fish pens in aquaculture application has already been met.

APPENDIX: Comparison Among Wind Tunnel Tests, Towing Tank Tests and the Theoretical Calculations

The nets tested in the wind tunnel were also tested in the towing tank. This was done in order to correlate the coefficient of drag measured in air with that measured in water. The net panels were tested at an angle of 90^{o} to the flow to verify the validity of the wind tunnel tests. The criteria used in establishing the test speeds in the tank were based on Reynolds number similarity.

Tests Conducted on the Net Panels

Net panels A and B were tested in the towing tank at speeds between 2 and 4 knots, which are the actual trawling speeds encountered in trawling operations.

The values of C_D have been plotted in figure A.1. Shown on the same plots are the corresponding values of C_D obtained in the wind tunnel for nets A and B at an angle of 90^{o} to the flow. In both cases the agreement between the towing tank and wind tunnel tests are quite close, and we can conclude that the wind tunnel tests can be substituted for the tests in water, provided modern synthetic fibers are used in the construction of the nets.

Tests Conducted on the Conical Nets

The conical nets with circular and elliptical openings were tested in the towing tank at the same speeds as the net panels. The net with a circular opening had the same geometric characteristics as those of net A. The geometry of the net with an elliptical opening is different than either of the two net panels tested.

Table A.1 gives the drag forces acting on the nets alone. The drag force measurements are shown in figures A.2 and A.3 for the circular and the elliptical nets. On the same graphs the drag

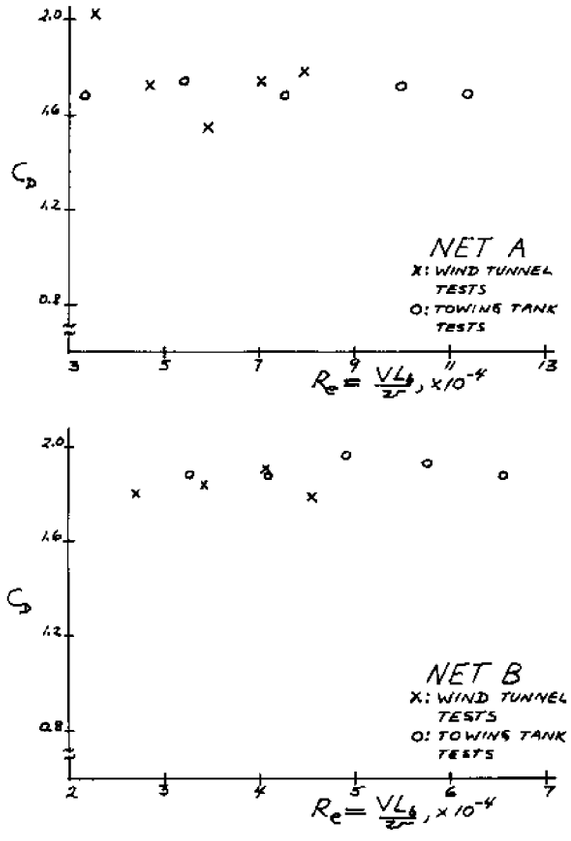

Figure A.1. Comparison of drag coefficients in air and water.

TABLE A.1. Drag forces acting on the nets alone.

V(ft/sec)	Circular D(lbf)	Elliptical D(lbf)
3.38	0.82	3.52
4.23	1.15	6.85
5.07	2.36	7.3
5.92	2.89	11.33
6.76	3.87	13.62

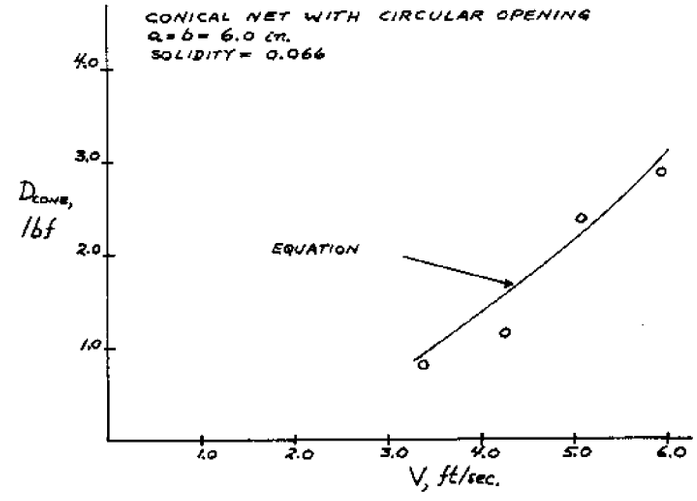

Figure A.2. Drag force vs. speed for the conical net with circular opening tested in the towing tank.

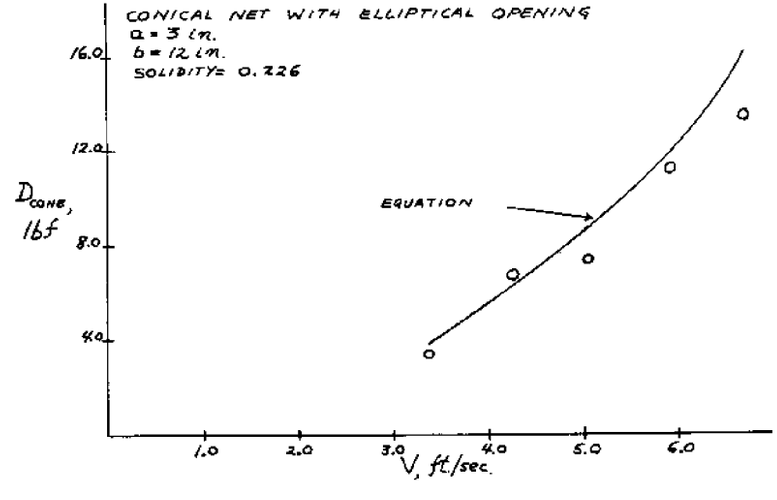

Figure A.3. Drag force vs. speed for the conical net with elliptical opening tested in the towing tank.

force predicted by equations 12 and 13 has been plotted. As in the case of the wind tunnel tests, there is good agreement between measurements and theory.

When comparing the values of coefficient of drag of the nets tested in air and in water, there are some critical factors to consider in addition to the requirement that the Reynolds number be the same.

The twine used to manufacture nets has the ability to shrink, expand and change its weight due to water absorption. Consequently, before accepting the values of C_D measured in the wind tunnel, some consideration must be given to the physical characteristics of the twine material. If the twine has a high degree of absorption, the added weight of the absorbed water will increase the drag of the panel. Another possibility is that the twine can change size in wet tests so that dry tests in the wind tunnel will take place at a changed dimension of bar lengths and knot diameters.

In the specific case of the netting panels and conical nets tested in this study these problems were practically non-existent. The twine making up the nets was Polyamide, more commonly known as nylon. Iitaka (1966) has measured the degrees of absorption and shrinkage of this type of netting twine and has found that they are negligible. In fact, most twine materials used in present commercial net fabrication are synthetic fibers which exhibit the same low absorption and shrinkage characteristics of nylon.

It can be concluded that the resistance characteristics of modern nets can be studied in wind tunnels and towing tanks interchangeably, with the only requirement that the Reynolds number be the same for both conditions.

References

Carrothers, P.J.G., Foulkes, T.J., Connors, M.P., Walker A. G. (1969) Data on the Engineering Performance of Canadian East Coast Groundfish Otter Trawls , Fisheries Research Board of Canada Technical Report No. 125.

Hoerner, S. F. (1965) Fluid Dynamic Drag.

Lindsey, W. F. (1938) NACA Technical Report 619.

Iitaka, Y. (1966) Lecture notes on fishing gear materials, College of Fisheries, Navigation, Marine Engineering and Electronics, St. John's, Canada.